Biogeosciences
Discussions
Open Access
EGU

1 **Deposit feeding of a foraminifera from an Arctic methane seep site**

2 **and possible association with a methanotroph revealed by**

3 **transmission electron microscopy**

4 Christiane Schmidt[1,2,3], Emmanuelle Geslin[1], Joan M Bernhard[4], Charlotte LeKieffre[1,5], Mette

5 Marianne Svenning[2,6], Helene Roberge[1,7], Magali Schweizer[1], Giuliana Panieri[2]

6 [1]LPG, Laboratoire de Planétologie et de Géodynamique, Univ. Angers, Université de Nantes, CNRS, LPG, SFR
7 QUASAV, Angers, 49000, France

8 [2]CAGE, Centre for Arctic Gas Hydrate, Environment and Climate, UiT, The Arctic University of Norway, Tromsø,
9 9010, Norway

10 [3]ZMT, Leibniz Centre for Tropical Marine Research, Bremen, 28359, Germany

11 [4]Woods Hole Oceanographic Institution, Geology & Geophysics Department, Woods Hole, 02543, MA, USA

12 [5]Cell and Plant Physiology Laboratory, CNRS, CEA, INRAE, IRIG, Université Grenoble Alpes, Grenoble, 38054
13 France

14 [6]Department of Arctic and Marine Biology, UiT, The Arctic University of Norway, Tromsø, 9037, Norway

15 [7]Université de Nantes, CNRS, Institut des Matériaux Jean Rouxel, IMN, Nantes, 44000 France

16

17 *Correspondence to* Christiane Schmidt christiane.schmidt@leibniz-zmt.de

18

19

Abstract. Several foraminifera are deposit feeders that consume organic detritus (dead particulate organic material along with entrained bacteria). However, the role of such foraminifera in the benthic food-web remains understudied. As foraminifera may associate with methanotrophic bacteria, which are ^{13}C-depleted, feeding on them has been suggested to cause negative δ^{13}C values in the foraminiferal cytoplasm and/or calcite. To test whether the foraminiferal diet includes methanotrophs, we performed a short-term (1 d) feeding experiment with *Nonionellina labradorica* from an active Arctic methane-emission site (Storfjordrenna, Barents Sea) using the marine methanotroph *Methyloprofundus sedimenti*, and analyzed *N. labradorica* cytology via Transmission Electron microscopy (TEM). We hypothesized that *M. sedimenti* would be visible, as evidenced by their ultrastructure, in degradation vacuoles after this feeding experiment. Sediment grains (mostly clay) occurred inside one or several degradation vacuoles in all foraminifers. In 24% of the specimens from the feeding experiment degradation vacuoles also contained bacteria, although none could be confirmed to be the offered *M. sedimenti*. Observations of the area adjacent to the aperture after 20 h incubation revealed three putative methanotrophs, close to clay particles. These methanotrophs were identified based on internal characteristics such as a type I stacked intracytoplasmic membranes (ICM), storage granules (SG) and gram-negative cell walls (GNCW). Furthermore, *N. labradorica* specimens were examined for specific adaptations to this active Arctic methane-emission site; we noted the absence of bacterial endobionts in all specimens examined but confirmed the presence of kleptoplasts, which were often partially degraded. Based on these observations, we suggest that *M. sedimenti* can be consumed by *N. labradorica* via untargeted grazing in seeps and that *N. labradorica* can be generally classified as a deposit feeder at this Arctic site. These results suggest that if methanothrophs are available to the foraminifera in their habitat, their non-selective uptake could make a substantial contribution to altering $\delta^{13}C_{test}$ values. This in turn may impact metazoans grazing on benthic foraminifera by altering their δ^{13}C signature.

benthic foraminifera – feeding experiment – grazing - marine methanotrophs – Arctic methane seeps– transmission electron microscopy – ultrastructure – kleptoplasts- protist – molecular identification

1. Introduction

50
51 In methane seep sites, the upward migration of methane affects the pore-water chemistry of near-
52 surface sediments, where benthic foraminifera inhabiting the sediment interface have been shown
53 to live (e.g. Dessandier et al., 2019). Extremely light isotopic signals of $\delta^{13}C$ have been measured
54 in seep-associated foraminiferal calcite tests (Wefer et al., 1994; Rathburn et al., 2003; Hill et al.,
55 2004b; Panieri et al., 2014). One explanation of low $\delta^{13}C$ signals in foraminifera could be due to
56 the ingestion of ^{13}C-depleted methanotrophs (Mccorkle et al., 1990; Wefer et al., 1994; Rathburn
57 et al., 2003; Panieri, 2006). Recently, specimens of the foraminifer *Melonis barleeanus*
58 (Williamson, 1858) collected from an active methane seep site were closely associated with
59 putative methanotrophs at their apertural region (Bernhard and Panieri, 2018).

60 The observation by Bernhard and Panieri (2018) brought to light the need to examine feeding
61 habits of foraminifera living on or around methane seeps. The species *M. barleeanus* could feed
62 on aerobic methane-oxidizing bacteria (methanothrophs), which are abundant in the water column
63 around methane seeps (Tavormina et al., 2010). Methanotrophs produce the biomarker diplopterol,
64 which has an extremely light $\delta^{13}C$ signature ($- 60$ ‰) and makes methanotrophs isotopically very
65 light themselves (Hinrichs et al., 2003). If foraminifera accidentally or intentionally ingest
66 methanotroph, $\delta^{13}C$ values of foraminiferal cytoplasm should be altered by such phagocytosis.
67 However, experimental evidence was inconclusive whether isotope labelling of food can influence
68 foraminiferal calcite, as no new calcite was produced during experiments using the foraminifera
69 *Haynesina germanica* and *Ammonia beccari* (Mojtahid et al., 2011). Experiments using a novel
70 high-pressure incubator on *Cibicides wuellerstorfi* illustrated the difficulty to measure the
71 relationship between methane exposure, $\delta^{13}C_{DIC}$ and $\delta^{13}C_{test}$, as whole cores were incubated, the
72 $\delta^{13}C_{DIC}$ of the seawater was impossible to keep constant and to compare $\delta^{13}C_{test}$ formed in the
73 presence of methane to normal marine conditions (Wollenburg et al., 2015).

74 Several studies found that the lightest isotopic $\delta^{13}C$ values were measured in tests coated by
75 methane-derived authigenic carbonate (MDAC) overgrowth (Torres et al., 2010; Panieri et al.,
76 2014; Consolaro et al., 2015; Panieri et al., 2017; Schneider et al., 2017). MDACs represent a
77 diagenetic alteration of the foraminiferal test that alters the $\delta^{13}C$ of the foraminiferal isotope record
78 It can form high-Mg-calcite coatings contributing to the bulk of foraminiferal carbonate up to 58
79 wt% MgCO (Schneider et al., 2017). MDACs are formed at the SMTZ, the sulfate-methane-
80 transition zone (SMTZ), near the sediment-water interface where the upward flow of methane

81 encounters the downward diffusion of sulfate from overlying seawater (Bian et al., 2001;

82 Schneider et al., 2017).

83 Light $\delta^{13}C$ values of foraminiferal calcite have been explained as being formed in the presence of

84 methane as an active uptake of methane-derived carbon produced by anaerobic oxidation of

85 methane (AOM) (Rathburn et al., 2003; Hill et al., 2004a; Panieri et al., 2014). Within the zone of

86 active AOM, the Dissolved Inorganic Carbon (DIC) exhibits the maximum ^{13}C-depletion

87 (Whiticar, 1999; Ussler and Paull, 2008).One hypothesis to explain extremely light $\delta^{13}C$ values

88 recorded in benthic foraminiferal calcite is that foraminifera assimilate the carbon as ^{13}C-depleted

89 methane-derived DIC, which would lead to extremely light $\delta^{13}C$ values. The possibility that ^{13}C-

90 depleted DIC from the pore water can be assimilated by foraminifera is currently debated. Some

91 studies suggest it is not possible (Herguera et al., 2014)   while others assert feasibility if

92 foraminifera calcify close to seeps (Rathburn et al., 2003; Hill et al., 2004a; Panieri et al., 2014).

93 However, light $\delta^{13}C$ values remain in many tests after MDACs are removed (Panieri et al., 2014)

94 and have been measured also in primary calcite, without MDACs, from tests in methane-rich

95 environments (e.g.Mackensen, 2008; Dessandier et al., 2019). These observations again point to

96 the role of food organisms influencing the cytoplasmatic $\delta^{13}C$ and could be incorporated into the

97 geochemistry of the test.

98 Foraminifera play an important role in the carbon cycle on the deep seafloor (Nomaki et al., 2005)

99 where feeding behavior and food preference vary with species (Nomaki et al., 2006). Selected

100 species of deep-sea benthic foraminifera have been shown to feed selectively on ^{13}C-labeled algae

101 from sedimentary organic matter, but unselectively on ^{13}C-labeled bacteria of the strain *Vibrio*

102 (Nomaki et al., 2006). A study from the seafloor around Adriatic seeps suggested that $\delta^{13}C$ of

103 foraminiferal cytoplasm could be influenced by feeding on the sulfur-oxidizing bacterium

104 *Beggiatoa,* whose abundance was also positively correlated with foraminiferal densities Panieri,

105 (Panieri, 2006). Generally, foraminifera can ingest dissolved organic matter (DOM), some are

106 herbivorous, carnivorous, suspension feeders and most commonly deposit feeders reviewerd in

107 (Lipps, 1983). Deposit feeders are omnivorous, gathering fine-grained sediment (e.g., clay) and

108 associated bacteria, organic detritus (dead particulate organic material) and, if present, diatom cells

109 using their pseudopodia. Hence, bacteria are involuntarily part of the "food-mix" (Levinton, 1989).

110 The fact that bacteria are sometimes part of the "food mix" made us investigate if *Nonionellina*

111 *labradorica* associated with methanotrophs, e.g. *Metyloprofundus sedimenti*, in a short-term

112   feeding experiment. *Nonionellina labradorica* is a benthic foraminifera that can reach substantial

113   sizes, is an abundant species in the North Atlantic, and is the northern-most species of the

114   Nonionellidae (Cedhagen, 1991). It also occurs together with *N. digitata* in Svalbard fjord

115   sediments (Hald and Korsun, 1997; Shetye et al., 2011; Fossile et al., 2020). The genus *Nonionella*

116   is potentially capable to denitrify, which as demonstrated on the species *Nonionella* cf. *stella*

117   (Risgaard-Petersen et al., 2006), and NIS *Nonionella* sp. T1 (Choquel et al., 2021), and has been

118   speculated also for *Nonionellina labradorica* (reviewed (Charrieau et al., 2019).Next to its wide

119   distribution, it is an especially interesting experimental species, because it hosts kleptoplasts, *i.e.*

120   sequestered chloroplasts, of diatom origin inside its cytoplasm (Cedhagen, 1991; Jauffrais et al.,

121   2018). SEM images of *N. labradorica*'s aperture show a specific ornamentation, possibly a

122   morphological adaptation to this "predatory" mode of life for obtaining the kleptoplasts (Bernhard

123   and Bowser, 1999). It is speculated that in deep-sea specimens the function of kleptoplasts is rather

124   related to the sulfur cycle rather than with photosynthesis (Jauffrais et al., 2019). Our study does

125   not concentrate on kleptoplasts but rather analyzed feeding preferences and contents of the

126   degradation vacuoles of this species from an active methane-emitting site in the Arctic

127   (Storfjordrenna, Barents Sea).

128

129   **2. Materials and methods**

130   **2.1. Site description and sampling living foraminifera**

131   The sampling site was located app. 50 km south of Svalbard at 382m water depth at the mouth of

132   Storfjordrenna (Serov et al., 2017). The site is characterized by several large gas hydrate pingos

133   (GHP), which actively vent methane spread over an area of 2.5 km^2. At this site our sample was

134   taken at GHP3 is referred as an underwater gas hydrate-bearing mound (Hong et al., 2017; Hong

135   et al., 2018). GHP3 is a ~500-m diameter, 10-m tall mound that actively vents methane (Fig. 1).

136   Marine sediment samples were collected during CAGE cruise 18-05 supported by the research

137   vessel *Kronprins Haakon* on in October 2018 and sampled from the seafloor by the Remotely

138   Operated Vehicle (ROV) Ægir. A blade corer (surface dimensions 27 x 19 cm, Fig. 1c) was used

139   to sample living foraminifera; it was placed directly in the vicinity of bacterial mats. The blade

140   corer containing the sediment sample was opened immediately once onboard. A small aquarium

141   hose was used to sample the upper most surface layer (0-1 cm). The wet sediment was collected

142   in petri dishes and wet sieved to a size range of 250-500 μm, which served as source of living

143   (cytoplasm containing) foraminifera. The species *N. labradorica,* which was the visibily

144   abundant, was subsequently used for feeding experiments described in detail below. A previous

145   study on GHP1 in Storfjordrenna showed also *N. labradorica* is also occuring in other sediment

146   cores (MC_902 and MC_919) in the top 2 cm (Carrier et al., 2020).
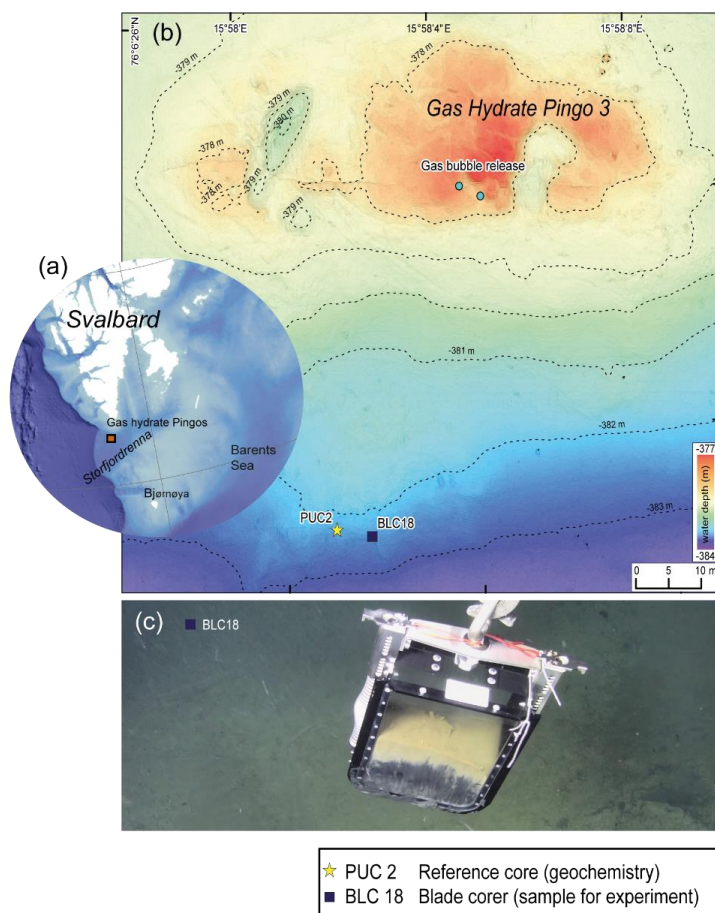
147

Figure 1 Description of the sampling site Gas hydrate Pingo 3 (GHP3), a gas-hydrate bearing mount, which actively vents methane, located in Storfjordrenna Barents Sea (a) Map illustrating Svalbard archipelago and the distance towards the sampling site is app. 50 km (b) Map of sampling site GHP3, active gas bubble release is marked on the top of the underwater mount, yellow star indicates location of push corer PUC2 taken for geochemical analysis, black squared box indicates the location of the blade corer BLC18 from which the sediment was derived for the experiment. (c) Underwater image of retrieval of BLC18 taken by camera of ROV (remotely operated vehicle) illustrating the coloration of sediment and the sea-floor visible in background.

Biogeosciences

Discussions

148 **2.2. Geochemistry**

149 For geochemical analysis a push corer (PUC2) was used (referred to as geochemistry core) to

150 obtain measurements on $\delta^{13}C_{DIC}$ and sulfate, as blade corer (BLC18) did not allow those

151 measurements. PUC2 was taken in close vicinity to BLC18, ~5m apart (Fig 1). Pore-water samples

152 were taken from PUC2 using rhizons that were inserted through pre-drilled holes in the core tube

153 at intervals of 1 cm. Acid washed 20-ml syringes were attached to the rhizons for pore water

154 collection. Depending on the amount of pore water collected, the samples were split for $\delta^{13}C_{DIC}$

155 and sulfate measurements. To the samples 10 µL of saturated $HgCl_2$ (aq) was added to stop

156 microbial activity, and stored in cold conditions (5°C). $\delta^{13}C_{DIC}$ was determined using a

157 ThermoScientific Gasbench II coupled to a ThermoScientific MAT 253 IRMS at the Stable Isotope

158 Laboratory (SIL) at CAGE, UiT. Anhydrous phosphoric acid was added to small glass vials

159 (volume 4.5 mL), that were closed and flushed with helium 5.0 gas before the pore water sub-

160 sample was measured. A pore-water sub-sample (volume 0.5 mL) was then added through the

161 septa with a syringe, followed by equilibration for 24 h at 24°C to liberate the CO_2 gas. Three solid

162 calcite standards with a range of +2 to -49 ‰ were used for normalization to $\delta^{13}C$ -VPDB.

163 Correction of measured $\delta^{13}C$ by -0.1 ‰, was done to account for fractionation between (g) and

164 (aq) in sample vials. Instrument precision for $\delta^{13}C$ on a MAT253 IRMS was 1σ +/- 0.1 ‰. Sulfate

165 was measured with a Metrohm ion chromatography instrument equipped with column Metrosep

166 A sup 4, and eluted with 1.8 mmol/L Na_2CO_3 + 1.7mmol/L $NaHCO_3$ at the University of Bergen.

167 **2.3. Culturing of the marine methanotroph *M. sedimenti***

168 *Methyloprofundus sedimenti* PKF-14 had been previously isolated from a water-column sample

169 collected at Prins Karls Forland, Svalbard in the laboratory at UiT in Tromsø. *Methyloprofundus*

170 *sedimenti* were cultured in 10-ml batches of a 35:65 mix of 1/10 Nitrate Mineral Salt medium

171 (NMS) and sterile filtered sea water using 125-mL Wheaton® serum bottles with butyl septa and

172 aluminum crimp caps (Teknolab®). Methane was injected to give a headspace of 20% methane in

173 air, and the bottles were incubated without shaking at 15°C in darkness. Purity of the cultures and

174 cell integrity was verified by microscopy and by absence of growth on agar plates with a general

175 medium for heterotrophic bacteria (tryptone, yeast extract, glucose and agar).

176 Transmission Electron Microscopy was performed on culture aliquots to allow morphological

177 comparison to previously published work (Tavormina et al., 2015). *Methyloprofundus sedimenti*

178 strain PKF-14 cells have a gram-negative cell wall, coccoid to slightly elongated shape and

179 characteristic stacked intracytoplasmic membrane (ISM) and storage granules (SG) (Fig 2c).

180 Additionally,16S rRNA gene sequencing was performed (data not shown) to confirm it to be

181 similar to the published *Methyloprofundus sedimenti* (Tavormina et al., 2015).

2.4. Experimental setup

183 On the ship, *Nonionellina labradorica* (Fig. 2) specimens showing a dark greenish brown

184 cytoplasm were picked using sable artist brushes under a stereomicroscope immediately after wet

185 sieving the sediment using natural seawater delivered from the ship pump. Living specimens had

186 a partly inorganic covering surrounding the test, which was gently removed using fine artist

187 brushes. Another Nonionellidae, *Nonionella iridea,* was similarly embedded with a cyst / covering

188 in sediment

189 Our specimens were subsequently rinsed twice in filtered artificial seawater to remove any

190 sediment before placing them into the experimental petri dishes. Care was taken that those were

191 minimally exposed to light during preparation of the experiment, as kleptoplasts are known to be

192 highly light sensitive in this foraminifer (Jauffrais et al., 2018).

193 The 20-h feeding experiment with *M. sedimenti* started after a short starvation phase where

194 organisms resided in petri dishes with ASW for 2-4 h and were not fed or manipulated during this

195 time. The feeding experiment consisted of several small petri dishes (3.5 cm ∅, 3 mL) each

196 containing five foraminifera in ASW at ambient salinity 35 (Red Sea Salt). Petri dishes were sealed

197 with Parafilm® and covered with aluminum foil and placed inside the incubator in complete

198 darkness. Temperature inside the chamber was maintained at 2-3°C, which is within the range of

199 the site's bottom-water temperature (-1.8 – 4.6°C) (Hong et al., 2017). The feeding of *M. sedimenti*

200 was performed once at the beginning of the experiment by adding 100 µL of culture to 3 mL of

201 artificial seawater to produce a final concentration of ~$1E10^6$ bacteria / mL in the experiment.

202 Previously conducted feeding studies were used as guides: Muller and Lee (1969) used $1El0^4$

203 bacteria/mL seawater and Mojtahid et al. (2011) used $4E10^8$ bacteria/mL seawater.

204 Five foraminifera, which served as initial/field specimens (Table 1), were fixed without *M.*

205 *sedimenti* incubation. The respective petri dishes, were incubated for 4, 8 and 20 h to determine if

206 incubation duration influenced response of the foraminifera to the methanotroph. One petri dish

207 containing five foraminifera, which were un-fed and fixed at 20 h, served as a negative "control".

208 After the end of the respective incubation times, each foraminifer was picked with a sterilized fine

8

209   artist brush, which was cleaned in 70% ethanol between each specimen, and placed individually

210   into a fixative solution (4% glutaraldehyde and 2% paraformaldehyde dissolved in ASW).
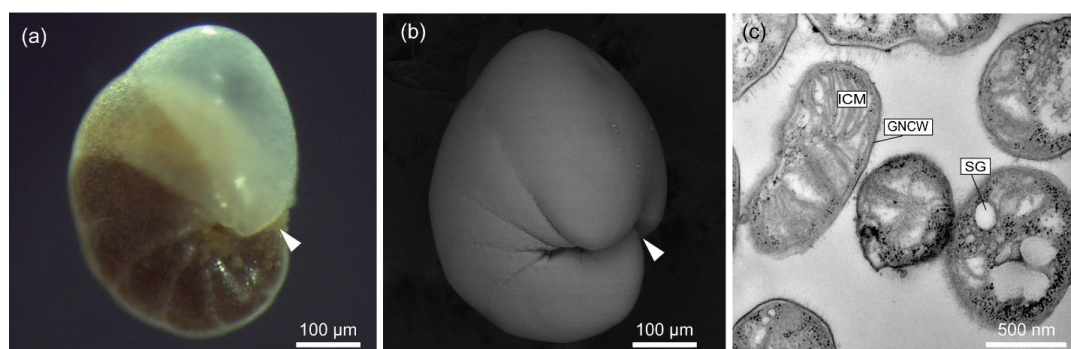

Figure 2 Exemplary illustration of *Nonionellina labradorica*, utilized in this study. (a) Reflected light microscopy image from a specimen directly after sampling, white arrowhead indicates aperture location (b) Scanning electron image from a specimen before molecular analysis was performed, white arrowhead indicates aperture location. (c) Transmission electron microscopy image of a culture of *Metyloprofundus sedimenti*, the marine methanotroph used in the feeding experiment. Characteristic features for methanotroph identification include typical type I ICM=intracytoplasmic membranes, SG=storage granules, and GNCW=gram-negative cell wall

211   **2.5. Transmission Electron microscopy (TEM) preparation**

212   Samples preserved in fixative solution were transported to the University of Angers, where they

213   were prepared for ultrastructural analysis using established protocols (Lekieffre et al., 2018).

214   Embedded foraminiferal cells were sectioned using an ultramicrotome (Leica® Ultracut S)

215   equipped with a diamond knife (Diatome®, ultra 45°). Grids were stained using UranyLess® EM

216   Stain (EMS, USA). Ultra-thin sections (70 nm) were observed with a JEOL JEM-1400 TEM at

217   the SCIAM facility, University of Angers.

218   To document the ultrastructure of *Methyloprofundus sedimenti*, a sub-sample of the culture used

219   for experiments was imaged with TEM (Fig. 2). To do so, an exponentially growing culture was

220   collected, centrifuged, pre-fixed with 2.5 % (w/v) glutaraldehyde in growth medium overnight,

221   washed in PBS (Phosphate Buffered Saline), then post fixed with 1% (w/v) aqueous osmium

222   tetroxide for 1. 5 hours at room temperature. After dehydration in an ethanol series, the samples

223   were embedded in an Epon equivalent (Serva) epoxy resin. Ultra-thin sections were cut on a Leica

224   EM UC6 ultramicrotome, and stained with 3 % (w/v) aqueous uranyl acetate followed by staining

225   with lead citrate (Reynolds, 1963) at 20 °C for 4–5 min. The samples were examined with a JEOL

226 JEM-1010 transmission electron microscope at an accelerating voltage of 80 kV with a Morada

227 camera system at the Advanced Microscopy Core Facility (AMCF), Faculty of Health Science,

228 UiT The Arctic University of Norway.

229 2.6. Foraminifera ultrastructural observation and image processing

230 Four specimens per experimental time point (4-20 h) plus one un-fed (control) specimen were

231 examined. From each specimen, a minimum of 50 TEM images was taken, including images

232 detailing the degradation vacuoles (5-27 images of degradation vacuoles per specimen). The

233 ultrastructure was examined at different parts of the images focusing (a) in the cell interior to

234 document vitality, (b) on degradation vacuoles to determine their content, and (c) at the exterior to

235 survey for microbes entrained in remnant "reticulopodial trunk" material, which can be extended

236 outside foraminiferal tests during feeding and locomotion (Anderson and Lee, 1991). Images are

237 deposited at PANGAEA with DOI number XXX. To obtain an overview of the entire specimen

238 and localize putative methanotrophs at the test (shell) aperture, images were compiled

239 automatically using the stitching-feature in Adobe Photoshop CS2.

240 2.7. Molecular genetics and morphology

241 DNA metabarcoding and morphological documentation were performed on 13 specimens of *N.*

242 *labradorica*. Briefly, live specimens were dried on micropaleontological slides and transported in

243 a small container, cooled with ice-pads to the University of Angers. All specimens were imaged

244 for morphological analysis using a Scanning Electron Microscope (SEM; EVOLS10, ZEISS, Fig.

245 S1) followed by individually extracting total DNA in DOC buffer (Pawlowski, 2000). To amplify

246 foraminiferal DNA, a hot start PCR (2 min. at 95°C) was performed in a volume of 25μl with 40

247 cycles of 30 s at 95°C, 30 s at 50°C and 2 min at 72°C, followed by 10 min at 72°C for final

248 extension. Primers s14F3 and sB were used for the first PCR and 30 cycles at an annealing

249 temperature of 52°C (other parameters unchanged) for the nested PCR with primers s14F1 and J2

250 (Pawlowski, 2000; Darling et al., 2016). Positive amplifications were sequenced directly with the

251 Sanger method at Eurofins Genomics (Cologne, Germany). For taxonomic identification, DNA

252 sequences were compared first with BLAST (Basic Local Alignment Search Tool) (Altschul et al.,

253 1997) and then within an alignment comprising other Nonionids implemented in SeaView (Gouy

254 et al., 2010) and corrected manually.

3. Results

3.1. Sample description and geochemistry

The visual observation of the sediments within the blade corer BLC18 immediately after sampling (Fig. 1) indicated that the sediment appears light grey – yellowish in the upper part until app. 13 cm and dark brown from app. 13 cm to the bottom. At approximately 13 cm the sulfate measured in the pore water of the geochemistry core (PUC2) declined from ~2750 ppm at the sediment-water interface to ~706 ppm. A decline in sulfate concentration indicates that the anaerobic oxidation of methane (AOM) occurred at app. 13 cm depth. The SMTZ (Sulfate Methane Transition Zone) characterized by a reduced δ^{13}C-DIC -32‰ at app. 13 cm sediment depth can be considered shallow on the global average (Egger et al., 2018).

3.2. Ultrastructure of methanotroph culture used in the feeding experiment

Metyloprofundus sedimenti is characterized by a typical type I intracellular stacked membrane (ISM), storage granules (SG) and typical gram-negative cell wall (GNCW) (Fig. 2). These features were used to identify *M. sediment*.

3.3. Foraminiferal ultrastructure from an Arctic seep environment

3.3.1 General ultrastructure

All 17 specimens were considered living at the time of observation (Fig. 3), as the mitochondria had characteristic double membranes and occasionally visible cristae (Nomaki et al., 2016). Cytoplasm exhibited several vacuoles and kleptoplasts concentrated in the youngest chambers (Fig. 3a) and, in some specimens, the nucleus with nucleoli was visible (Fig. 3b). Kleptoplasts were numerous throughout the cytoplasm and occurred in the form of a single chloroplast (Fig. 3a-b), or as double chloroplasts (Fig. S2). Not all kleptoplasts were intact, some showed peripheral degradation of the membranes indicated by an increasing number of white areas between pyrenoid, lamella and thylakoids (Fig. S2). Peroxisomes in *N. labradorica* occurred mostly as pairs (Fig. 3c) or small clusters of 3-4 spherical organelles (Fig. S1a-b). The mitochondria occurred often in small clusters of two to five throughout the cytoplasm and were oval, round or kidney-shaped in cross section (Fig. 3e-f). Sometimes, but not always, peroxisomes were associated with endoplasmic reticulum (Fig. S1c) but could also occur alone. Golgi apparatus (Fig 3d) had intact membranes, often occurring near mitochondria.
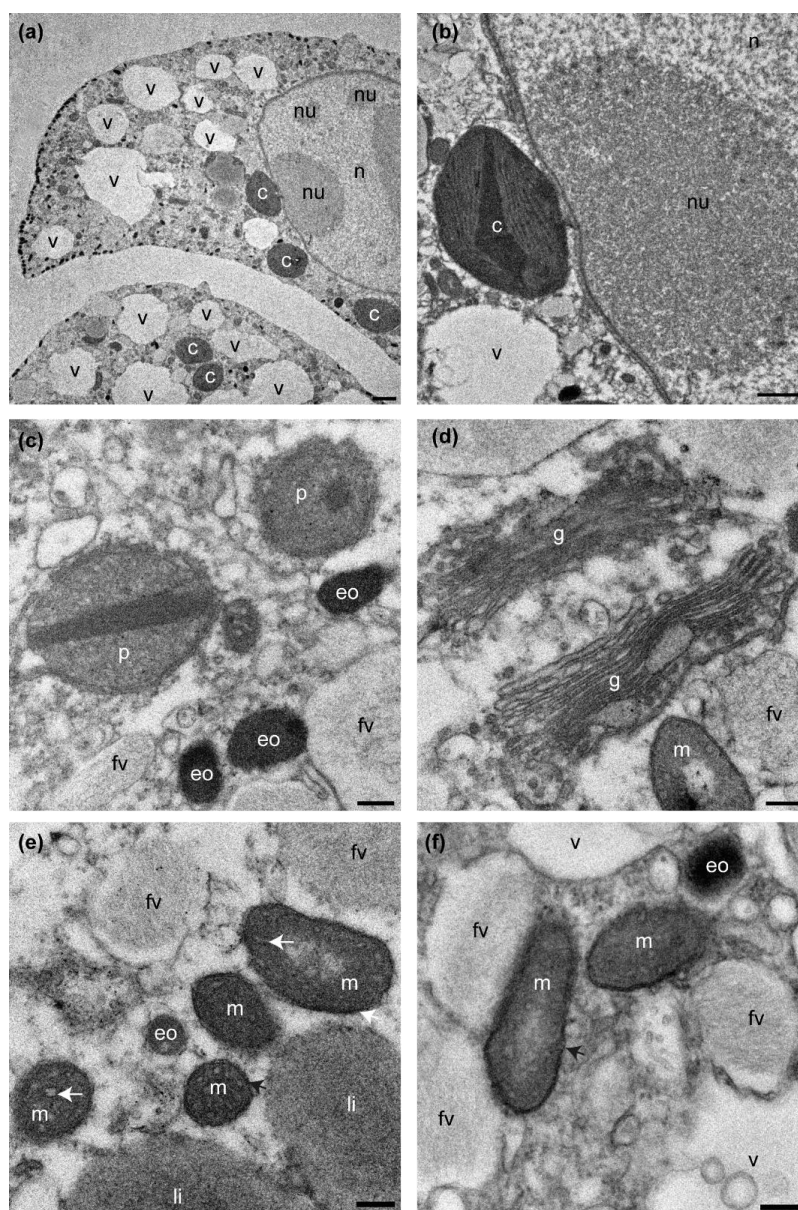
286

Figure 3 Transmission electron micrographs showing cellular ultrastructure of *N. labradorica*. (a) Cytoplasm showing parts of two chambers, with nucleus with nucleoli, vacuoles and several kleptoplasts, (b) nuclear envelope, nucleoli, and kleptoplasts, (c) peroxisomes and electron opaque bodies, (d) Golgi, (e-f) mitochondria. v=vacuole, c=kleptoplast, nu=nucleoli, n=nucleus p=peroxisome, eo=electron opaque body, m=mitochondrion, fv=fibrillar vesicle, li=lipid droplet. Scales: (a) 2 μm, (b) 1 μm, (c-f) 200 nm

3.3.2 Ultrastructure of aperture-associated bacteria

In total three putative methanotrophs were identified in the vicinity of two foraminifer specimens (sample E39, Fig. 4; E37, Fig. 5). Those were identified next to reticulopodial remains in the cross-section (Fig. 4b). As an aid for identification of *M. sedimenti* we used the characteristics shown in the literature (Tavormina et al. 2015) and a our own TEM observation obtained from *M. sedimenti* culture (Fig. 2c). As noted, *Methyloprofundus sedimenti* is characterized by a typical type I intracellular stacked membrane (ISM), storage granules (SG) and typical gram-negative cell wall (GNCW) (Fig. 2). On specimen E39 from the 20 h treatment, we found the methanotroph exhibiting the clearest internal structure, having both typical type I stacked intracytoplasmic membranes (ICM+SG) and a second putative methanotroph showing SG+GNCW (Fig. 4). Specimen E36, from the 20 h treatment, hosted another putative methanotroph showing three large SG (Fig. 5). Storage granules occur throught this putative methanotroph (Fig. 5c).
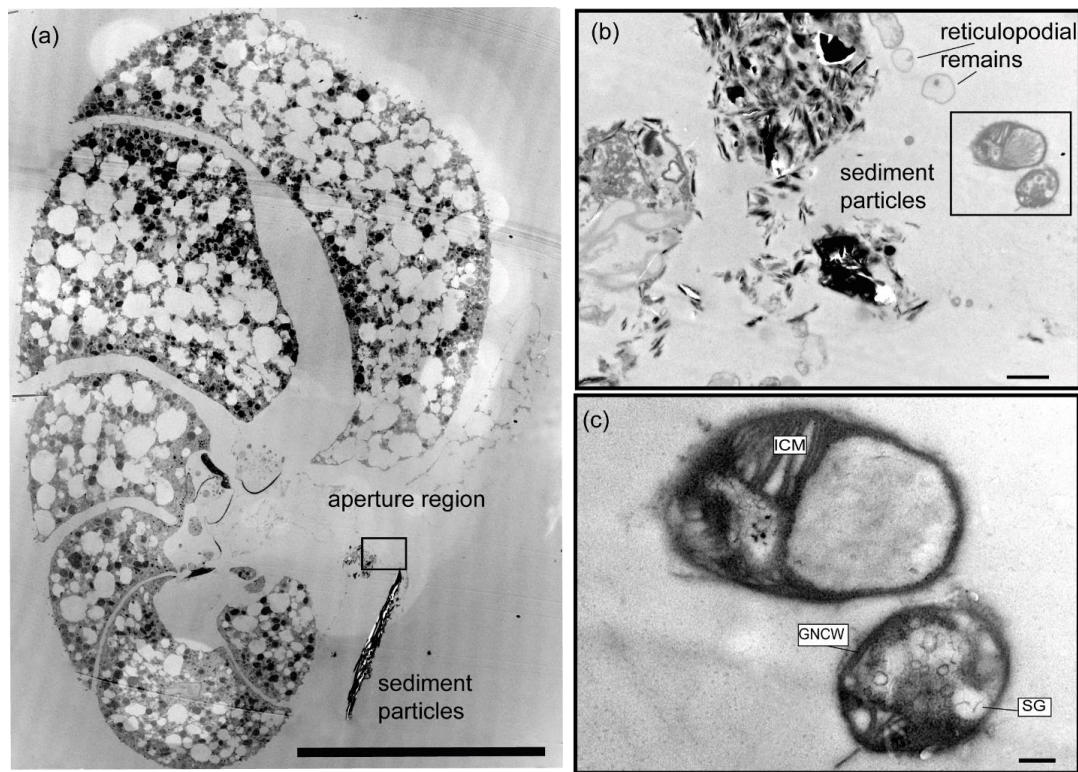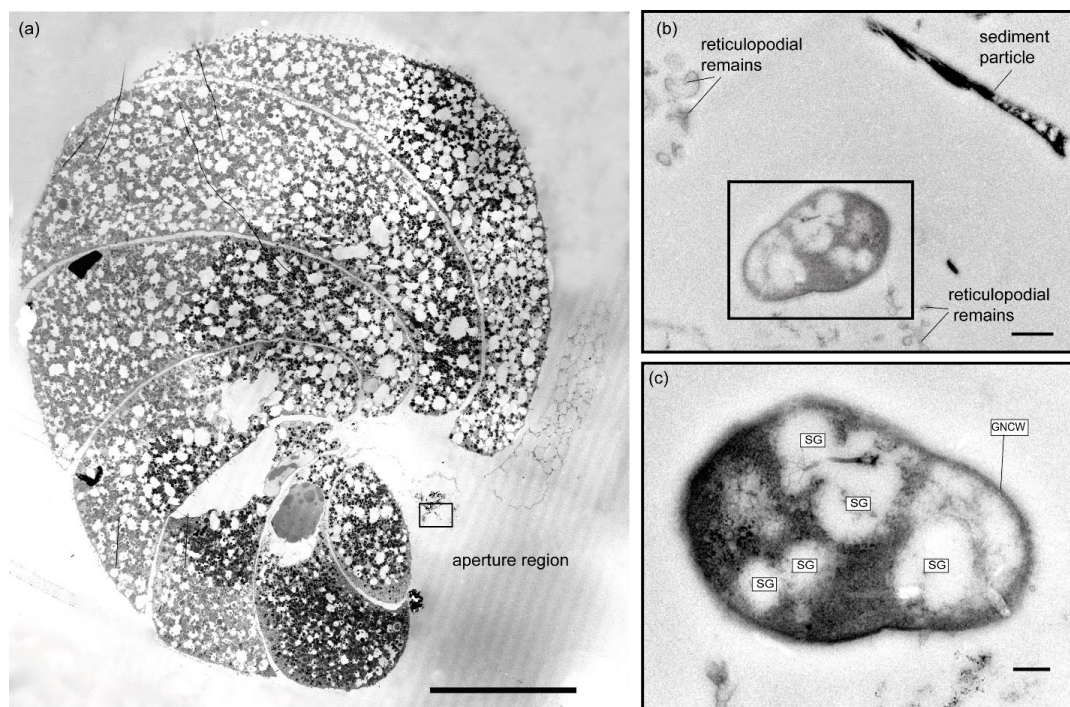
302

Figure 4 Transmission electron micrographs of *N. labradorica* from 20 h treatment (sample E39) (a) Stitched cross section of TEM images showing location of methanotroph at the aperture region (black rectangle) (b) Location of two putative methanotrophs next to sediment particles and putative reticulopodial remains. (c) Close up of two putative methanotrophs revealing detailed feature for identification, such as stacked membranes (ISM), storage granules (SG), and gram-negative cell wall (GNCW), scale bars: a: 100 μm, b: 1 μm, c: 200 nm.

Figure 5 Transmission electron micrographs of *N. labradorica* from 20 h treatment (sample E37) (a) Stitched cross section of TEM images showing location of putative methanotroph (black rectangle) at the aperture region. (b) Location of the putative methanotroph next to sediment particles and sections of the putative reticulopodial remains (c) Close up of putative methanotroph showing several SG throughout its cell, scale bars: a: 100 µm, b: 0.5 µm, c: 200 nm.

3.3.3 Contents degradation vacuoles

Digestive vacuoles and food vacuoles are often summarized as degradation vacuoles in the literature (Lekieffre et al., 2018) and this makes sense for our study as well. A degradation vacuole is a vacuole where enzymatic activities degrade contents, often making them unidentifiable (Bé et al., 1982; Hemleben et al., 2012). Sediment particles were present in many degradation vacuoles. The sediment grains are easy to recognize in the TEM image as angular grains spiking out of the vacuoles, next to organic debris, which can have many different shapes. Each specimen had at least one degradation vacuole with sediment particles present (Table 1). If a sediment particle was visible, the vacuole was defined as a degradation vacuole (dv), and if it was not then it was defined as a standard vacuole (v) (Fig. 6). Sediment particles are likely the remains of clay grains from the seafloor, and hence show that the vacuole must contain cell foreign objects, around which degradation processes have started. Next to sediment particles, 4 out of 17 specimens examined (23%) had a few bacteria of various sizes inside their degradation vacuoles (Fig 6 b-c).
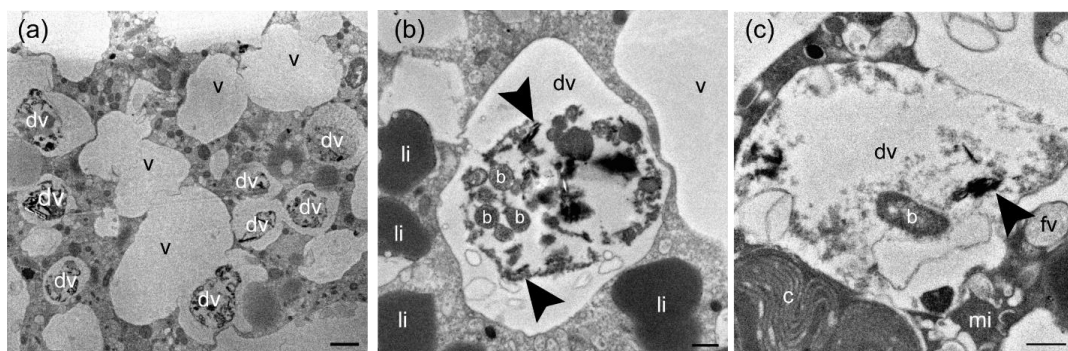
15

318

Figure 6 TEM micrographs of N. labradorica. (a) Overview of degradation vacuoles (dv) in relation to empty vacuoles (v) in the youngest chambers of specimen E5 (field). (b) Bacteria in degradation vacuoles (white b) next to clay particles (black arrow) in specimen E14 (8 h incubation). (c) Elongated bacterium inside degradation vacuole adjacent to clay particles of specimen E37 (20 h incubation), scale bars: a: 2 µm, b,c: 0.5 µm.

319 **3.4. Foraminiferal genetics**

320 Six of 13 specimens analyzed for genetics were positively amplified and sequenced (Fig. S3). The

321 sequences are deposited in GenBank under the accession numbers MN514777 to MN514782.

322 When comparing them via BLAST, they were between 98.6% and 99.6% identical to published

323 sequences belonging to foraminifera identified as the morphospecies *N. labradorica*, from the

324 Skagerrak, Svalbard and the White Sea (Holzmann and Pawlowski, 2017; Jauffrais et al., 2018).

325 Sequences were also included in an alignment comprising other nonionids implemented in

326 Seaview (not shown) and corrected manually to check the BLAST search. This step confirmed the

327 BLAST identification.

328
329
330
331

332 **4. Discussion**

333 4.1. Sampling site and geochemistry

334 The sampling site of blade corer BLC18 was in close proximity (~50 m) to an active methane-vent

335 releasing methane bubbles at the gas hydrate Pingo (GHP3) (Serov et al., 2017). At such sites with

336 high methane flux, the SMTZ (sulfate methane transition zone) is shallow, as sulfate from the

337 sediment is readily consumed in the first tens of (Barnes and Goldberg, 1976; Iversen and

338 Jørgensen, 1993) by sulfate-reducing bacteria (SRB) (reviewed in Carrier et al., 2020).

339 Geochemical analysis of PUC2, revealed an SMTZ at app. 13 cm. The depth of 13 cm is rather

340 shallow (Egger et al., 2018), as it can also be several meters deep in other sites (reviewed in Panieri

341 et al., 2017). Geochemical characteristics can be considered similar at the sampling location of

342 living specimens (BLC18) and the core taken for geochemistry (PUC2).

343

344 4.2. Association with putative methanotrophs

345 The association with the three putative methanotrophs could be identified on two foraminifera

346 specimens based on comparing internal bacterial characteristics to published literature (Tavormina

347 et al., 2015). Transmission electron microscopy is a powerful tool to reveal ultrastructural features

348 outside of the foraminiferal cytoplasm. The documentation of this association with putative

349 methanotrophs likely originating from the food given in the experiment, is evidence that

350 methanotrophs can indeed be a food source to *N. labradorica*. The feeding strategy is likely that

351 methanotrophs are ingested via untargeted grazing in seeps, as *N. labradorica* appears to be a non-

352 selective feeder.

353 After conducting this study and comparing to the result of observations on *Melonis barleeanus*

354 (Bernhard and Panieri, 2018) an association of foraminifera and methanotrophs has been clearly

355 demonstrated. Whether foraminifera feed methanotrophs and under which environmental

356 conditions remains speculative. It has been shown that large scale biofilms of methanotrophs can

357 occur in sediment pockets close to the Sulfate Methane Transition Zone (SMTZ)(Gründger et al.,

358 2019). This is also the location where Anaerobic Oxidation of Methane (AOM) occurs (Boetius et

359 al., 2000). The SMTZ is characterized by sulfate reducing bacteria (SRB), and a consortium of

360 ANME that are driving the AOM (Boetius et al., 2000; Wegener et al., 2015). However,this is not

361 the main habitat for living foraminifera, as the SMTZ can be several meters deep and alters

362 foraminiferal tests with secondary overgrowths of methane-derived authigenic carbonates

363   (MDAC) (reviewed in Panieri et al., 2017). It has also been suggested that foraminifera may

364   sometimes be transported into seeps and can also occur at tze SMTZ, but they likely not live in

365   those sediment layers permanently(Bernhard and Bowser, 1999). Foraminfiera in general have

366   several metabolic strategies to cope with anoxic environments (Gomaa et al., 2021) of which many

367   remain to be understudied.

368

369   4.3. Feeding on other bacteria and contents of degradation vacuoles

370   Our results of the feeding experiment and experimental specimens show that only 23% of the

371   examined *N. labradorica* specimens contained bacteria inside their degradation vacuoles. That is

372   not a large quantity compared to sediment particles which occurred in 100% of the examined

373   degradation vacuoles. We infer that *N. labradorica* at this site is a deposit feeder, feeding on

374   organic detritus and associated bacteria. The bacteria observed in the degradation vacuoles

375   resembled those from other deep-sea foraminifera (*Globobulimina pacifica* and *Uvigerina*

376   *peregrina*) and the shallow-dwelling genus *Ammonia* (Goldstein and Corliss, 1994). Salt-marsh

377   foraminifera also feed on bacteria and detritus, as observed in TEM studies (Frail-Gauthier et al.,

378   2019). Scavenging on bacteria has also been observed by other foraminifera from intertidal

379   environments such as *Ammonia tepida* or *Haynesina germanica* (Pascal et al., 2008) and is a

380   logical consequence from detritus feeding. Certain foraminifera have been shown to selectively

381   ingest algae/bacteria according to strain (Lee et al., 1966; Lee and Muller, 1973). From laboratory

382   cultures we know that several foraminifera cultures require bacteria to reproduce, as antibiotics

383   inhibited reproduction (Muller and Lee, 1969). Future studies will need to employ additionally

384   molecular tools to additionally determine the food contents inside the cytoplasm (e.g.(Salonen et

385   al., 2019). A recent study by used metabarcoding to assess the contribution of bacterial OTUs

386   associated with intertidal foraminifera, and revealed that *Ammonia* sp. T6 can predateon metazoan

387   taxa, whereas *Elphidium* sp. S5 and *Haynesina* sp. S16 are more likely to ingest diatoma

388   (Chronopoulou et al., 2019).

389

390   4.4. General ultrastructure of *N. labradorica* collected in a seep environment

391   Our observations also included the major organelles of the species, as this was essential to conclude

392   vitality after the experiment (Nomaki et al., 2016). Mitochondria were generally homogeneously

393   distributed throughout the cytoplasm confirming previous observations of six *N. labradorcia* from

394 the Gullmar Fjord (Jauffrais et al., 2018; Lekieffre et al., 2018). If mitochondria are concentrated

395 predominately under pore plugs, it can be an indicator that the electron acceptor oxygen is scarce

396 in their environment, as the pores are the direct connection from the cell to the environment. This

397 has been observed in several other studies where mitochondria were accumulated under pores in

398 *N. stella* (Leutenegger and Hansen, 1979) and *Bolivina pacifica* (Bernhard et al., 2010).

399 For the samples from our particular site, we also observed kleptoplasts abundantly and evenly

400 distributed throughout the cytoplasm, confirming previous TEM studies on the species from fjord

401 sediments (Cedhagen, 1991; Jauffrais et al., 2018). Occasionally, kleptoplasts were degraded,

402 which could happen a) during sampling, b) due to exposure to microscope lights or c) due to the

403 age and condition of kleptoplasts inside host. Kleptoplasts in *N. labradorica* have been studied in

404 detail describing their diatom origin, sensitivity to light and missing photosynthetic functionality

405 (e.g. (Cedhagen, 1991; Jauffrais et al., 2018). It has been suggested that kleptoplasts could function

406 as a seasonal energy reservoir (e.g. in winter) (Jauffrais et al., 2016).

407 **5. Conclusions**

408 Based on the content of degradation vacuoles observed, we conclude that *N. labradorica* is a

409 deposit feeder, as it ingests sediment particles together with bacteria as part of consuming detritus

410 on the sea floor. At the aperture region of two different foraminifera specimens, next to

411 reticulopodial remains and sediment particles, we observed three putative marine methanotrophs

412 after 20 h incubation. One of the putative methanotrophs had characteristic ISM, which resemble

413 the methanotroph *M. sedimenti* in culture. We conclude that it is possible that *N. labradorica*

414 ingests *M. sedimenti* via "untargeted grazing" in seeps. Further studies are needed on feeding

415 strategies of several paleo-oceanographically relevant foraminifera to detangle the relationship

416 between $\delta^{13}C$ measured in foraminiferal calcite, cytoplasm and contribution to their diet.

417

418 **6. Data availability**

419 Data in form of TEM images will be deposited at PANGAEA under doi:

420 Molecular data will be deposited before publication at Genbank.

421

422 **7. Sample availability**

423 Samples are available upon request and TEM thinsections archived at the University of Angers.

8. Acknowledgments

We thank the captains, crew members and scientists onboard R/V *Kronprins Haakon* and ROV Ægir Team for their assistance; Anne-Grethe Hestnes for growing the methanotroph culture. Florence Manero, Romain Mallet and Rodolphe Perrot at the SCIAM microscopy facility University of Angers are to thank for their expertise with the TEM and SEM. We thank Sunil Vadakkepuliyambatta for helping to prepare the map presented in Figure 1; Sophie Quinchard (LPG-BIAF) for supporting the molecular analysis. Funding was received through the Research Council of Norway, CAGE (Center for Excellence in Arctic Gas Hydrate Environment and Climate, project number 223259) and NORCRUST (project number 255150) to GP, EG, and CS. CS position was funded through the MOPGA (Make Our Planet Great Again) fellowship by CAMPUS France, the NORCRUST project and the University of Angers. JMB was partially supported by US NSF 1634469, WHOI's Investment in Science Program, and by the Région Pays de la Loire through the FRESCO Project.

Author Contributions

Designed the project and experiment: GP, EG, CS; Collected samples: CS, EG; Performed experiment: CS; Sample preparation: CS, HR; TEM observations and interpretations: CS, JMB, EG, CL; Conducted molecular genetics: MSc; Wrote the paper: CS, GP, JMB; Provided critical review and edits to the manuscript: EG, CL, MSv, MSc, HR; Contributed reagents/materials/analysis tools: MSv, MSc, CL.

444 **Table I.** Summary of TEM observations of *Nonionellina labradorica* comparing field specimens

445 and experimental specimens. Field specimens (initials) were not fed, nor was a non-fed control

446 preserved after a 20 h incubation. The only putative methanotrophs were observed and imaged in

447 specimens from the 20 h incubation. Bacteria of unknown origin were described as rod shaped

448 cells in the degradation vacuoles.

449

Duration of experiment (h)/field samples	Food provided (yes (x)/no)	Sample ID	Cytoplasm: Degradation vacuole Contents		Aperture region: (putative) Methanotrophs
			bacteria	Clay/in-organics	
Field samples (Initials)	No	E1	no	x	no
	No	E3	no	x	no
	No	E5	no	x	no
	No	E6	no	x	no
4	x	E25	no	x	no
	x	E27	x	x	no
	x	E28	no	x	no
	x	E29	no	x	no
8	x	E14	x	x	no
	x	E15	no	x	no
	x	E16	no	x	no
	x	E17	no	x	no
20	x	E36	x	x	1 x
	x	E37	x	x	no
	x	E38	no	x	no
	x	E39	no	x	2 x
Control (20)	no	E44	no	x	no

450

451

452

21

453 References :

454

455 Altschul, S. F., Madden, T. L., Schäffer, A. A., Zhang, J., Zhang, Z., Miller, W., and Lipman, D.
456 J.: Gapped BLAST and PSI-BLAST: a new generation of protein database search programs,
457 Nucleic Acids Res., 25, 3389-3402, https://doi.org/10.1093/nar/25.17.3389, 1997.

458 Anderson, O. and Lee, J.: Cytology and fine structure, in: Biology of Foraminifera, edited by:
459 Lee, J. J., Anderson, O.R., Academic Press, London, 7-40., 1991.

460 Barnes, R. O. and Goldberg, E. D.: Methane production and consumption in anoxic marine
461 sediments, Geology, 4, 297-300, https://doi.org/10.1130/0091-
462 7613(1976)4<297:MPACIA>2.0.CO;2, 1976.

463 Bé, A. W. H., Spero, H. J., and Anderson, O. R.: Effects of symbiont elimination and reinfection
464 on the life processes of the planktonic foraminifer Globigerinoides sacculifer, Marine Biology,
465 70, 73-86, https://doi.org/10.1007/BF00397298, 1982.

466 Bernhard, J. M. and Bowser, S. S.: Benthic foraminifera of dysoxic sediments: chloroplast
467 sequestration and functional morphology, Earth-Sci. Rev., 46, 149-165,
468 https://doi.org/10.1016/s0012-8252(99)00017-3, 1999.

469 Bernhard, J. M. and Panieri, G.: Keystone Arctic paleoceanographic proxy association with
470 putative methanotrophic bacteria, Sci Rep-Uk, 8, 10610, https://doi.org/10.1038/s41598-018-
471 28871-3, 2018.

472 Bernhard, J. M., Goldstein, S. T., and Bowser, S. S.: An ectobiont-bearing foraminiferan,
473 Bolivina pacifica, that inhabits microxic pore waters: cell-biological and paleoceanographic
474 insights, Environmental Microbiology, 12, 2107-2119, 10.1111/j.1462-2920.2009.02073.x,
475 2010.

476 Bian, L., Hinrichs, K.-U., Xie, T., Brassell, S. C., Iversen, N., Fossing, H., Jørgensen, B. B., and
477 Hayes, J. M.: Algal and archaeal polyisoprenoids in a recent marine sediment: Molecular
478 isotopic evidence for anaerobic oxidation of methane, Geochemistry, Geophysics, Geosystems,
479 2, https://doi.org/10.1029/2000GC000112, 2001.

480 Boetius, A., Ravenschlag, K., Schubert, C. J., Rickert, D., Widdel, F., Gieseke, A., Amann, R.,
481 Jørgensen, B. B., Witte, U., and Pfannkuche, O.: A marine microbial consortium apparently
482 mediating anaerobic oxidation of methane, Nature, 407, 623, https://doi.org/10.1038/35036572,
483 2000.

484 Carrier, V., Svenning, M. M., Gründger, F., Niemann, H., Dessandier, P.-A., Panieri, G., and
485 Kalenitchenko, D.: The Impact of Methane on Microbial Communities at Marine Arctic Gas
486 Hydrate Bearing Sediment, Frontiers in Microbiology, 11, 10.3389/fmicb.2020.01932, 2020.

487 Cedhagen, T.: Retention of chloroplasts and bathymetric distribution in the sublittoral
488 foraminiferan Nonionellina labradorica, Ophelia, 33, 17-30,
489 https://doi.org/10.1080/00785326.1991.10429739, 1991.

490 Charrieau, L. M., Ljung, K., Schenk, F., Daewel, U., Kritzberg, E., and Filipsson, H. L.: Rapid
491 environmental responses to climate-induced hydrographic changes in the Baltic Sea entrance,
492 Biogeosciences, 16, 3835-3852, 10.5194/bg-16-3835-2019, 2019.

493 Choquel, C., Geslin, E., Metzger, E., Filipsson, H. L., Risgaard-Petersen, N., Launeau, P.,
494 Giraud, M., Jauffrais, T., Jesus, B., and Mouret, A.: Denitrification by benthic foraminifera and
495 their contribution to N-loss from a fjord environment, Biogeosciences, 18, 327-341, 10.5194/bg-
496 18-327-2021, 2021.

497 Chronopoulou, P.-M., Salonen, I., Bird, C., Reichart, G.-J., and Koho, K. A.: Metabarcoding
498 insights into the trophic behavior and identity of intertidal benthic foraminifera, Frontiers in
499 microbiology, 10, 1169, https://doi.org/10.3389/fmicb.2019.01169, 2019.

500 Consolaro, C., Rasmussen, T., Panieri, G., Mienert, J., Bünz, S., and Sztybor, K.: Carbon isotope
501 ($\delta 13C$) excursions suggest times of major methane release during the last 14 kyr in Fram Strait,
502 the deep-water gateway to the Arctic, Clim. Past, 11, 669-685, https://doi.org/10.5194/cp-11-
503 669-2015, 2015.

504 Darling, K. F., Schweizer, M., Knudsen, K. L., Evans, K. M., Bird, C., Roberts, A., Filipsson, H.
505 L., Kim, J.-H., Gudmundsson, G., Wade, C. M., Sayer, M. D. J., and Austin, W. E. N.: The
506 genetic diversity, phylogeography and morphology of Elphidiidae (Foraminifera) in the
507 Northeast Atlantic, Mar. Micropaleontol., 129, 1-23,
508 https://doi.org/10.1016/j.marmicro.2016.09.001, 2016.

509 Dessandier, P.-A., Borrelli, C., Kalenitchenko, D., and Panieri, G.: Benthic Foraminifera in
510 Arctic Methane Hydrate Bearing Sediments, Frontiers in Marine Science, 6,
511 https://doi.org/10.3389/fmars.2019.00765, 2019.

512 Egger, M., Riedinger, N., Mogollón, J. M., and Jørgensen, B. B.: Global diffusive fluxes of
513 methane in marine sediments, Nature Geoscience, 11, 421-425, 10.1038/s41561-018-0122-8,
514 2018.

515 Fossile, E., Nardelli, M. P., Jouini, A., Lansard, B., Pusceddu, A., Moccia, D., Michel, E., Péron,
516 O., Howa, H., and Mojtahid, M.: Benthic foraminifera as tracers of brine production in
517 Storfjorden "sea ice factory", Biogeosciences, 17, https://doi.org/10.5194/bg-17-1933-2020,
518 2020.

519 Frail-Gauthier, J. L., Mudie, P. J., Simpson, A. G. B., and Scott, D. B.: Mesocosm and
520 Microcosm Experiments On the Feeding of Temperate Salt Marsh Foraminifera, J. Foraminifer.
521 Res., 49, 259-274, https://doi.org/10.2113/gsjfr.49.3.259, 2019.

522 Goldstein, S. T. and Corliss, B. H.: Deposit feeding in selected deep-sea and shallow-water
523 benthic foraminifera, Deep Sea Research Part I: Oceanographic Research Papers, 41, 229-241,
524 https://doi.org/10.1016/0967-0637(94)90001-9, 1994.

525 Gomaa, F., Utter, D. R., Powers, C., Beaudoin, D. J., Edgcomb, V. P., Filipsson, H. L., Hansel,
526 C. M., Wankel, S. D., Zhang, Y., and Bernhard, J. M.: Multiple integrated metabolic strategies
527 allow foraminiferan protists to thrive in anoxic marine sediments, Science Advances, 7,
528 eabf1586, doi:10.1126/sciadv.abf1586, 2021.

529 Gouy, M., Guindon, S., and Gascuel, O.: SeaView version 4: a multiplatform graphical user
530 interface for sequence alignment and phylogenetic tree building, Mol. Biol. Evol., 27, 221-224,
531 https://doi.org/10.1093/molbev/msp259, 2010.

532 Gründger, F., Carrier, V., Svenning, M. M., Panieri, G., Vonnahme, T. R., Klasek, S., and
533 Niemann, H.: Methane-fuelled biofilms predominantly composed of methanotrophic ANME-1 in
534 Arctic gas hydrate-related sediments, Sci Rep-Uk, 9, 9725, https://doi.org/10.1038/s41598-019-
535 46209-5, 2019.

536 Hald, M. and Korsun, S.: Distribution of modern benthic foraminifera from fjords of Svalbard,
537 European Arctic, The Journal of Foraminiferal Research, 27, 101-122,
538 https://doi.org/10.2113/gsjfr.27.2.101, 1997.

539 Hemleben, C., Spindler, M., and Anderson, O. R.: Modern planktonic foraminifera, Springer
540 Science & Business Media2012.

541 Herguera, J. C., Paull, C. K., Perez, E., Ussler Iii, W., and Peltzer, E.: Limits to the sensitivity of
542 living benthic foraminifera to pore water carbon isotope anomalies in methane vent
543 environments, Paleoceanography, 29, 273-289, https://doi.org/10.1002/2013PA002457, 2014.

544 Hill, R., Schreiber, U., Gademann, R., Larkum, A. W. D., Kuhl, M., and Ralph, P. J.: Spatial
545 heterogeneity of photosynthesis and the effect of temperature-induced bleaching conditions in
546 three species of corals, Marine Biology, 144, 633-640, https://doi.org/10.1007/s00227-003-1226-
547 1, 2004a.

548 Hill, T. M., Kennett, J. P., and Valentine, D. L.: Isotopic evidence for the incorporation of
549 methane-derived carbon into foraminifera from modern methane seeps, Hydrate Ridge,
550 Northeast Pacific, Geochimica et Cosmochimica Acta, 68, 4619-4627,
551 https://doi.org/10.1016/j.gca.2004.07.012, 2004b.

552 Hinrichs, K.-U., Hmelo, L. R., and Sylva, S. P.: Molecular fossil record of elevated methane
553 levels in late Pleistocene coastal waters, Science, 299, 1214-1217,
554 https://doi.org/10.1126/science.1079601, 2003.

555 Holzmann, M. and Pawlowski, J.: An updated classification of rotaliid foraminifera based on
556 ribosomal DNA phylogeny, Mar. Micropaleontol., 132, 18-34,
557 https://doi.org/10.1016/j.marmicro.2017.04.002, 2017.

558 Hong, W.-L., Torres, M. E., Carroll, J., Crémière, A., Panieri, G., Yao, H., and Serov, P.:
559 Seepage from an arctic shallow marine gas hydrate reservoir is insensitive to momentary ocean
560 warming, Nat. Commun., 8, 15745, https://doi.org/10.1038/ncomms15745, 2017.

561 Hong, W. L., Torres, M. E., Portnov, A., Waage, M., Haley, B., and Lepland, A.: Variations in
562 gas and water pulses at an Arctic seep: fluid sources and methane transport, Geophys. Res. Lett.,
563 45, 4153-4162, https://doi.org/10.1029/2018GL077309, 2018.

564 Iversen, N. and Jørgensen, B. B.: Diffusion coefficients of sulfate and methane in marine
565 sediments: Influence of porosity, Geochimica et Cosmochimica Acta, 57, 571-578,
566 https://doi.org/10.1016/0016-7037(93)90368-7, 1993.

567 Jauffrais, T., LeKieffre, C., Schweizer, M., Jesus, B., Metzger, E., and Geslin, E.: Response of a
568 kleptoplastidic foraminifer to heterotrophic starvation: photosynthesis and lipid droplet
569 biogenesis, FEMS Microbiol. Ecol., 95, 10.1093/femsec/fiz046, 2019.

570 Jauffrais, T., LeKieffre, C., Schweizer, M., Geslin, E., Metzger, E., Bernhard, J. M., Jesus, B.,
571 Filipsson, H. L., Maire, O., and Meibom, A.: Kleptoplastidic benthic foraminifera from aphotic
572 habitats: Insights into assimilation of inorganic C, N, and S studied with sub-cellular resolution,
573 Environmental Microbiology, 0, https://doi.org/10.1111/1462-2920.14433, 2018.

574 Lee, J. J. and Muller, W. A.: Trophic dynamics and niches of salt marsh foraminifera, Am. Zool.,
575 13, 215-223, 1973.

576 Lee, J. J., McEnery, M., Pierce, S., Freudenthal, H., and Muller, W.: Tracer experiments in
577 feeding littoral foraminifera, The Journal of Protozoology, 13, 659-670, 1966.

578 LeKieffre, C., Bernhard, J. M., Mabilleau, G., Filipsson, H. L., Meibom, A., and Geslin, E.: An
579 overview of cellular ultrastructure in benthic foraminifera: New observations of rotalid species in
580 the context of existing literature, Mar. Micropaleontol., 138, 12-32,
581 https://doi.org/10.1016/j.marmicro.2017.10.005, 2018.

582 Leutenegger, S. and Hansen, H. J.: Ultrastructural and radiotracer studies of pore function in
583 foraminifera, Marine Biology, 54, 11-16, 10.1007/BF00387046, 1979.

584 Levinton, J. S.: Deposit feeding and coastal oceanography, in: Ecology of marine deposit
585 feeders, Springer, 1-23, 1989.

586 Lipps, J. H.: Biotic Interactions in Benthic Foraminifera, in: Biotic Interactions in Recent and
587 Fossil Benthic Communities, edited by: Tevesz, M. J. S., and McCall, P. L., Springer US,
588 Boston, MA, 331-376, 10.1007/978-1-4757-0740-3_8, 1983.

589 Mackensen, A.: On the use of benthic foraminiferal δ13C in palaeoceanography: constraints
590 from primary proxy relationships, Geological Society, London, Special Publications, 303, 121-
591 133, https://doi.org/10.1144/SP303.9, 2008.

592 McCorkle, D. C., Keigwin, L. D., Corliss, B. H., and Emerson, S. R.: The influence of
593 microhabitats on the carbon isotopic composition of deep-sea benthic foraminifera,
594 Paleoceanography, 5, 161-185, https://doi.org/10.1029/PA005i002p00161, 1990.

595 Mojtahid, M., Zubkov, M. V., Hartmann, M., and Gooday, A. J.: Grazing of intertidal benthic
596 foraminifera on bacteria: Assessment using pulse-chase radiotracing, J. Exp. Mar. Biol. Ecol.,
597 399, 25-34, https://doi.org/10.1016/j.jembe.2011.01.011, 2011.

598 Muller, W. A. and Lee, J. J.: Apparent Indispensability of Bacteria in Foraminiferan Nutrition,
599 The Journal of Protozoology, 16, 471-478, https://doi.org/10.1111/j.1550-7408.1969.tb02303.x,
600 1969.

601 Nomaki, H., Heinz, P., Nakatsuka, T., Shimanaga, M., and Kitazato, H.: Species-specific
602 ingestion of organic carbon by deep-sea benthic foraminifera and meiobenthos: In situ tracer
603 experiments, Limnol. Oceanogr., 50, 134-146, https://doi.org/10.4319/lo.2005.50.1.0134, 2005.

604 Nomaki, H., Heinz, P., Nakatsuka, T., Shimanaga, M., Ohkouchi, N., Ogawa, N. O., Kogure, K.,
605 Ikemoto, E., and Kitazato, H.: Different ingestion patterns of C-13-labeled bacteria and algae by
606 deep-sea benthic foraminifera, Marine Ecology-Progress Series, 310, 95-108,
607 https://doi.org/10.3354/meps310095, 2006.

608 Nomaki, H., Bernhard, J. M., Ishida, A., Tsuchiya, M., Uematsu, K., Tame, A., Kitahashi, T.,
609 Takahata, N., Sano, Y., and Toyofuku, T.: Intracellular Isotope Localization in Ammonia sp.
610 (Foraminifera) of Oxygen-Depleted Environments: Results of Nitrate and Sulfate Labeling
611 Experiments, Frontiers in Microbiology, 7, https://doi.org/10.3389/fmicb.2016.00163, 2016.

612 Panieri, G.: Foraminiferal response to an active methane seep environment: A case study from
613 the Adriatic Sea, Mar. Micropaleontol., 61, 116-130,
614 https://doi.org/10.1016/j.marmicro.2006.05.008, 2006.

615 Panieri, G., James, R. H., Camerlenghi, A., Westbrook, G. K., Consolaro, C., Cacho, I., Cesari,
616 V., and Cervera, C. S.: Record of methane emissions from the West Svalbard continental margin
617 during the last 23.500yrs revealed by δ13C of benthic foraminifera, Global and Planetary
618 Change, 122, 151-160, https://doi.org/10.1016/j.gloplacha.2014.08.014, 2014.

619 Panieri, G., Lepland, A., Whitehouse, M. J., Wirth, R., Raanes, M. P., James, R. H., Graves, C.
620 A., Crémière, A., and Schneider, A.: Diagenetic Mg-calcite overgrowths on foraminiferal tests in
621 the vicinity of methane seeps, Earth and Planetary Science Letters, 458, 203-212,
622 https://doi.org/10.1016/j.epsl.2016.10.024, 2017.

623 Pascal, P.-Y., Dupuy, C., Richard, P., and Niquil, N.: Bacterivory in the common foraminifer
624 Ammonia tepida: Isotope tracer experiment and the controlling factors, J. Exp. Mar. Biol. Ecol.,
625 359, 55-61, https://doi.org/10.1016/j.jembe.2008.02.018, 2008.

626 Pawlowski, J.: Introduction to the molecular systematics of foraminifera, Micropaleontology, 46,
627 1-12, 2000.

628 Rathburn, A. E., Pérez, M. E., Martin, J. B., Day, S. A., Mahn, C., Gieskes, J., Ziebis, W.,
629 Williams, D., and Bahls, A.: Relationships between the distribution and stable isotopic
630 composition of living benthic foraminifera and cold methane seep biogeochemistry in Monterey
631 Bay, California, Geochemistry, Geophysics, Geosystems, 4,
632 https://doi.org/10.1029/2003GC000595, 2003.

633 Risgaard-Petersen, N., Langezaal, A. M., Ingvardsen, S., Schmid, M. C., Jetten, M. S. M., Op
634 den Camp, H. J. M., Derksen, J. W. M., Piña-Ochoa, E., Eriksson, S. P., Peter Nielsen, L., Peter
635 Revsbech, N., Cedhagen, T., and van der Zwaan, G. J.: Evidence for complete denitrification in a
636 benthic foraminifer, Nature, 443, 93, https://doi.org/10.1038/nature05070, 2006.

637 Salonen, I. S., Chronopoulou, P.-M., Bird, C., Reichart, G.-J., and Koho, K. A.: Enrichment of
638 intracellular sulphur cycle–associated bacteria in intertidal benthic foraminifera revealed by 16S
639 and aprA gene analysis, Sci Rep-Uk, 9, 1-12, https://doi.org/10.1038/s41598-019-48166-5, 2019.

640 Schneider, A., Crémière, A., Panieri, G., Lepland, A., and Knies, J.: Diagenetic alteration of
641 benthic foraminifera from a methane seep site on Vestnesa Ridge (NW Svalbard), Deep Sea
642 Research Part I: Oceanographic Research Papers, 123, 22-34,
643 https://doi.org/10.1016/j.dsr.2017.03.001, 2017.

644 Serov, P., Vadakkepuliyambatta, S., Mienert, J., Patton, H., Portnov, A., Silyakova, A., Panieri,
645 G., Carroll, M. L., Carroll, J., Andreassen, K., and Hubbard, A.: Postglacial response of Arctic
646 Ocean gas hydrates to climatic amelioration, Proceedings of the National Academy of Sciences,
647 114, 6215-6220, 10.1073/pnas.1619288114, 2017.

648 Shetye, S., Mohan, R., Shukla, S. K., Maruthadu, S., and Ravindra, R.: Variability of
649 Nonionellina labradorica Dawson in Surface Sediments from Kongsfjorden, West Spitsbergen,
650 Acta Geologica Sinica - English Edition, 85, 549-558, https://doi.org/10.1111/j.1755-
651 6724.2011.00450.x, 2011.

652 Tavormina, P. L., Ussler, W., Joye, S. B., Harrison, B. K., and Orphan, V. J.: Distributions of
653 putative aerobic methanotrophs in diverse pelagic marine environments, The ISME Journal, 4,
654 700-710, https://doi.org/10.1038/ismej.2009.155, 2010.

655 Tavormina, P. L., Hatzenpichler, R., McGlynn, S., Chadwick, G., Dawson, K. S., Connon, S. A.,
656 and Orphan, V. J.: Methyloprofundus sedimenti gen. nov., sp. nov., an obligate methanotroph
657 from ocean sediment belonging to the 'deep sea-1'clade of marine methanotrophs, Int. J. Syst.
658 Evol. Microbiol., 65, 251-259, https://doi.org/10.1099/ijs.0.062927-0, 2015.

659 Torres, M. E., Martin, R. A., Klinkhammer, G. P., and Nesbitt, E. A.: Post depositional alteration
660 of foraminiferal shells in cold seep settings: New insights from flow-through time-resolved
661 analyses of biogenic and inorganic seep carbonates, Earth and Planetary Science Letters, 299,
662 10-22, https://doi.org/10.1016/j.epsl.2010.07.048, 2010.

663 Ussler, W. and Paull, C. K.: Rates of anaerobic oxidation of methane and authigenic carbonate
664 mineralization in methane-rich deep-sea sediments inferred from models and geochemical
665 profiles, Earth and Planetary Science Letters, 266, 271-287,
666 https://doi.org/10.1016/j.epsl.2007.10.056, 2008.

667 Wefer, G., Heinze, P. M., and Berger, W. H.: Clues to ancient methane release, Nature, 369, 282,
668 https://doi.org/10.1038/369282a0, 1994.

669 Wegener, G., Krukenberg, V., Riedel, D., Tegetmeyer, H. E., and Boetius, A.: Intercellular
670 wiring enables electron transfer between methanotrophic archaea and bacteria, Nature, 526, 587-
671 590, 10.1038/nature15733, 2015.

672 Whiticar, M. J.: Carbon and hydrogen isotope systematics of bacterial formation and oxidation of
673 methane, Chemical Geology, 161, 291-314, https://doi.org/10.1016/S0009-2541(99)00092-3,
674 1999.

675 Wollenburg, J. E., Raitzsch, M., and Tiedemann, R.: Novel high-pressure culture experiments on
676 deep-sea benthic foraminifera—Evidence for methane seepage-related $\delta 13C$ of Cibicides
677 wuellerstorfi, Mar. Micropaleontol., 117, 47-64, 2015.
678